Analytical Modelling of Current-Voltage Characteristics of Ballistic Graphene Nanoribbon Field-Effect Transistors

George S. Kliros
Department of Aeronautical Sciences, Division of Electronics and Communication Engineering
Hellenic Air-Force Academy, Dekeleia Air-Force Base GR-1010, Attica, Greece.
Email: gskliros@ieee.org

***Abstract*—We present an analytical model for the I-V characteristics of Grephene Nanoribbon Field Effect Transistors (GNR-FETs) based on effective mass approximation and semiclassical ballistic transport. The model incorporates the effects of edge bond relaxation and third nearest neighbor (3NN) interaction as well as thermal broadening. Several performance metrics of double-gate GNR-FETs, operating close to quantum capacitance limit, are calculated. Numerical results show that AGNRs with widths of about 3-4 nm at most are required in order to obtain optimum high frequency and switching performance.**

I. Introduction

Graphene, has recently emerged as a potential candidate for nanoelectronics since its high mobility and carrier velocity promises ballistic devices with high switching speeds [1]. Interestingly, if graphene is patterned into nanoribbons, using planar technologies such as electron beam lithography and etching, a sizeable bandgap opens. Son et. al. [2] have shown that the band gap of an armchair GNR (AGNR) arises from both the quantum confinement and the edge effects. As a consequence, FETs with AGNR channels (AGNR-FETs), showing complete switch off and improved on-off current ratios, can be considered as building blocks for future digital circuits. Numerical modelling of GNR-FETs is usually based on a 'top-of-the barrier' approach under ballistic transport [3]. More accurate 'atomistic' models are based on self-consistent non-equilibrium Green's Function (NEGF) formalism in some cases including GNRs edge effects [4]. However, atomistic numerical models are computationally expensive and motivate the need for analytical modelling [5]. In this work, we present a fully analytical model for the I-V characteristics of ballistic Grephene Naanoribbon FETs based on effective mass approximation and semiclassical ballistic transport. Effective mass approximation is well suited for describing narrow GNRs since their band dispersion curves are approximately parabolic. The model incorporates the effects of edge bond relaxation and 3NN-interaction as well as thermal broadening. To investigate the performance metrics of GNR-FETs, analytical expressions are provided for the charge density, quantum capacitance as well as drain current as functions of gate voltage. Since significant performance improvement is expected in the quantum capacitance limit QCL [6], a double-gate AGNR-FET (Fig.1) operating close to QCL, is investigated.

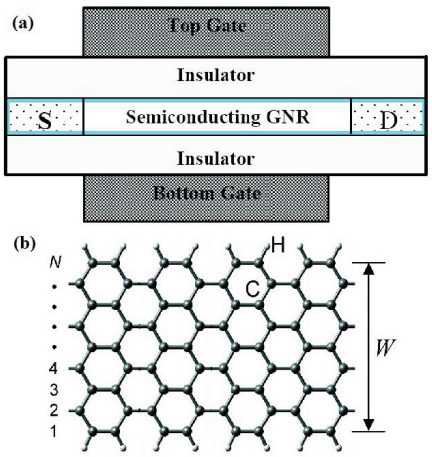

Fig. 1. (a) Schematics of double-gate GNR FET where a semiconducting AGNR is used as channel material. (b) The atomic structure of an AGNR.

II. Analytical Model

In order to develop an analytical model based on the effective mass approximation, we first need an expression for the energy band structure of AGNRs. It has been verified that a 3NN tight binding model incorporating the edge-bond relaxation can accurately predict the band structure of GNRs [7]. Using a Taylor expansion around the charge neutrality point, the band structure of an AGNR can be written as

$$E_n^{\pm}(k_x) = \pm\sqrt{E_{C,n}^2 + (\hbar\upsilon_n k_x)^2} \tag{1}$$

with

$$E_{C,n} = \gamma_1\left(1 + 2scos(n\theta)\right) + \gamma_3\left(1 + 2scos(2n\theta)\right) + \frac{4(\gamma_3 + \Delta\gamma_1)}{N+1} sin^2(n\theta) \tag{2}$$

and

$$(\hbar\upsilon_n)^2 = (3a_{cc})^2\Big[-\frac{1}{2}s\gamma_1 cos(n\theta) \times \left(\gamma_1 + \gamma_3(1 + 2cos(2n\theta) + \frac{4(\gamma_3 + \Delta\gamma_1)}{N+1} sin^2(n\theta)\right) - \gamma_3\left(\gamma_1 + 2\gamma_3 cos(2n\theta) + \frac{4(\gamma_3 + \Delta\gamma_1)}{N+1} sin^2(n\theta)\right)\Big] \tag{3}$$

978-1-4673-5736-4/13/$31.00 ©2013 IEEE

where $\theta = \pi/(N+1)$, $\pm$ indicates the conduction band and valence band respectively, N is the total number of carbon atoms in the transverse direction, n denotes the subband index, and $E_{C,n}$ is the band edge energy of the nth subband. Due to the symmetric band structure of electrons and holes, one obtains for the energy gap $E_{G,n} = 2E_{C,n}$. Also, $\gamma_1 = -3.2eV$ and $\gamma_3 = -0.3eV$ refer to the first and third-nearest neighbor hopping parameters and $\Delta\gamma_1 = -0.2eV$ is used for the correction to γ_1 due to edge bond relaxation effect.

The electron effective masses at the bottom of the conduction band is given by $m_n^* = E_{C,n}/v_n^2$ and the energy gap is $E_{G,n} = 2E_{C,n}$. Assuming a ballistic channel, the carrier density inside the channel is given by [8]

$$n_{1D} = \sqrt{\frac{k_B T}{2\pi\hbar^2}} \sum_{n>0} \sqrt{m_n^*} \left[F_{-1/2}(\eta_{n,S}) + F_{-1/2}(\eta_{n,D}) \right] \tag{4}$$

where $F_{1/2}$ is the Fermi-Dirac integral of order $-1/2$, $\eta_{n,S} = (E_{FS} - E_{C,n})/k_B T$ and $\eta_{n,D} = (E_{FD} - E_{C,n})/k_B T$. Moreover, the following relation between the gate voltage and the source Fermi energy $E_{FS} = E_F$ can be obtained [8]

$$V_G(E_F) - V_{FB} = \frac{E_F}{q} + \frac{q n_{1D}(E_F)}{C_{ins}} \tag{5}$$

where q is the carrier charge, C_{ins} is the gate-insulator capacitance per unit length of the GNR and V_{FB} denotes the flat-band voltage. The gate-insulator capacitance per unit length can be calculated by [9]

$$C_{ins} = N_G \kappa \epsilon_0 \left(\frac{W}{t_{ins}} + \alpha \right) \tag{6}$$

where N_G is the number of gates, κ is the relative dielectric constant of the gate insulator, t_{ins} is the gate-insulator thickness and $\alpha \simeq 1$ is a dimensionless fitting parameter.

The bias-dependent gate capacitance per unit length C_G can be modelled as a series combination of insulator capacitance C_{ins} per unit length and the quantum capacitance per unit length C_Q, that is,

$$C_G(V_G) = \frac{C_{ins} C_Q(E_F)}{C_{ins} + C_Q(E_F)} \tag{7}$$

where the quantum capacitance per unit length can be written in terms of Fermi integrals of order (-3/2),

$$C_Q = \frac{q^2}{(2\pi\hbar^2 k_B T)^{1/2}} \sum_{n>0} \sqrt{m_n^*} \left[F_{-3/2}(\eta_{n,S}) + F_{-3/2}(\eta_{n,D}) \right] \tag{8}$$

Finally, following Natori's ballistic theory [10],

$$I_D = \frac{q}{\pi\hbar} \sum_{n>0} \left[\int_{E_{C,n}}^{\infty} (f_S(E) - f_D(E)) dE \right] \tag{9}$$

After integrating, Eq.(9) yields

$$I_D = \frac{q k_B T}{\pi\hbar} \sum_{n>0} \ln \left(\frac{1 + exp(\eta_{n,S})}{1 + exp(\eta_{n,D})} \right) \tag{10}$$

In the above model, we assume that $C_G \gg C_D$ and $C_G \gg C_S$ which means that the gate has perfect electrostatic control over the channel. Moreover, carrier scattering by ion-impurities and electron-hole puddle effect [11] are not considered, assuming that such effects can be overcome by processing advancements in the future.

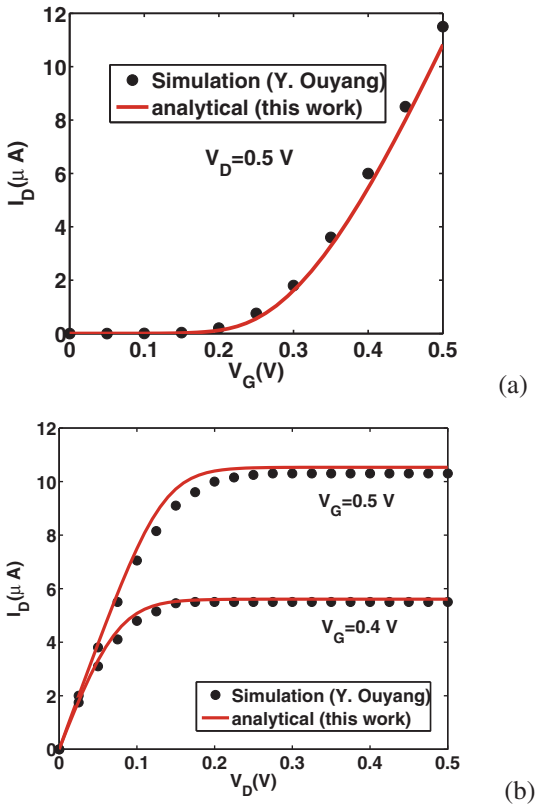

Fig. 2. Transfer $I_D - V_G$ (a) and output $I_D - V_D$ characteristics (b) simulated in Ref. [3] (dots) and calculated in this work (solid line).

III. Results and Discussion

Firstly, the validity of our analytical model is examined by comparing the calculated I-V characteristics with the corresponding ones of Ref. [3] based on a 'top of the barrier' model combined with a tight-binding numerical approach. The GNRFET considered in this comparative study, is a single gate transistor with an intrinsic AGNR channel of width 2.1 nm (N=18) and the gate insulator capacitance is $C_{ins} = 2pF/cm$. As it is seen from Figs. 2(a) and (b) good agreement is found for both transfer and output characteristics. Note that, 3NN-hopping is neglected here. Next, we investigate the $I-V$ characteristics of the double-gate AGNR-FET with gate-insulator HfO_2 of thickness $t_{ins} = 1$ nm and relative dielectric constant κ=16. Since thin and high-κ gate insulator is employed, we can expect excellent gate control to prevent source-drain direct tunneling. Moreover, the quantum capacitance limit (QCL), where the small quantum capacitance dominates the total gate capacitance, can be reached. Concerning the effect of edges on the band structure, we found that, in the presence of both edge bond relaxation all AGNRs are semiconducting with bandgaps well separated in to three different groups $N = 3p$, $N = 3p+1$, $N = 3p+2$. However, members of the family $N = 3p+2$ are not considered here as their bandgaps are too small to be useful as semiconductors. Therefore, we restrict our study to the families $N = 3p$ and $N = 3p+1$ that are more promising for FET applications having larger bandgaps. Figures 3(a),(b) and 3(c),(d) show the transfer characteristics $I_D - V_G$ as well as output characteristics $I_D - V_D$ for the two groups $N = 3p$ and $N = 3p+1$, respectively, where the

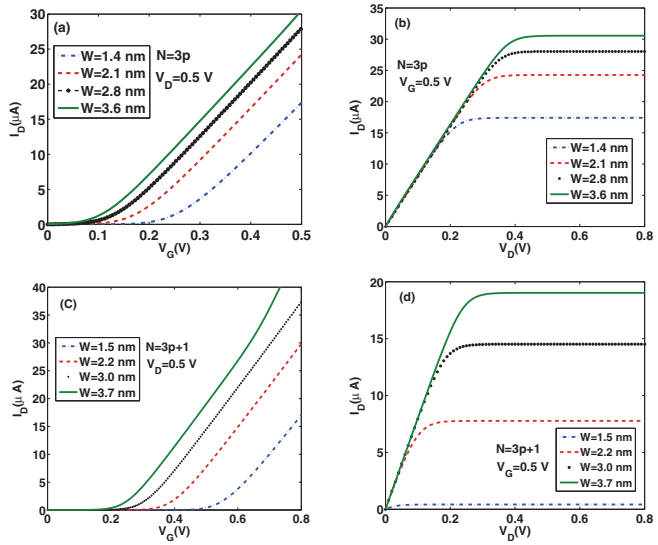

Fig. 3. Width dependence of the transfer and output characteristics for the families $N = 3p$ (a,b) and $N = 3p + 1$ (c,d) respectively.

results for several increasing widths are plotted together in each panel. As expected from the difference in the bandstructures, the characteristics show smaller values of threshold voltage and larger drain currents for the group $N = 3p$ compared to those of the group $N = 3p + 1$ with approximately the same width.

In order to assess the potential of AGNR-FETs in analog design, the transcoductance over current ratio (g_m/I_D) figure of merit has been calculated and ploted in Fig.4(a) and (b) for the families $N = 3p$ and $N = 3p + 1$ respectively. As it is seen, the family $N = 3p$ is less efficient in terms of g_m/I_D than family $N = 3p + 1$ showing significant degradation as the gate voltage is increased. Moreover, we assess the high frequency performance of the device under study. Once the transconductance g_m and gate capacitance C_G are calculated, the cutoff frequency can be computed as $f_T = g_m/(2\pi C_G)$ with $V_D = V_{DD}$. To understand the intrinsic performance we only consider the channel capacitance excluding the parasitic capacitances. Fig. 5(a) and (b) show the gate voltage dependence of the calculated f_T of a device with channel length $L_G = 50$ nm for the two groups $N = 3p$ and $N = 3p + 1$, respectively. A rather peaky behavior as function of gate voltage is observed similar to the existing FET technologies. As it is seen, AGNRs with $N = 3p$ have higher maximum cutoff frequencies obtained at lower gate biases and hence, are preferable for high frequency applications. A useful piece of information would be to see the width dependence of the cut-off frequency. As it is seen in Fig.6, f_T has a maximum value of 6.6 THz, around $W = 3$ nm, for the family $N = 3p$ and a maximum value of 4 THz, around $W = 4$ nm, for the family $N = 3p + 1$.

Finally, in order to assess the device performance for digital applications, the I_{on}/I_{off} ratio versus GNR's width and I_{on}/I_{off} is calculated and plotted in Fig.7. Although the on-current increases with increasing the width, the I_{on}/I_{off} ratio decreases. Moreover, the family $N = 3p$ is more efficient from the on-current performance point of view, but

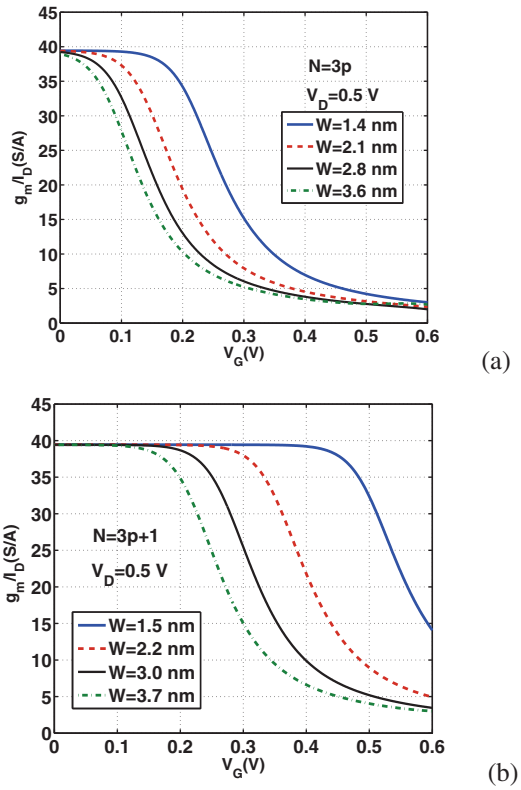

Fig. 4. g_m/I_D versus V_G for the families $N = 3p$ (a) and $N = 3p + 1$ (b), respectively.

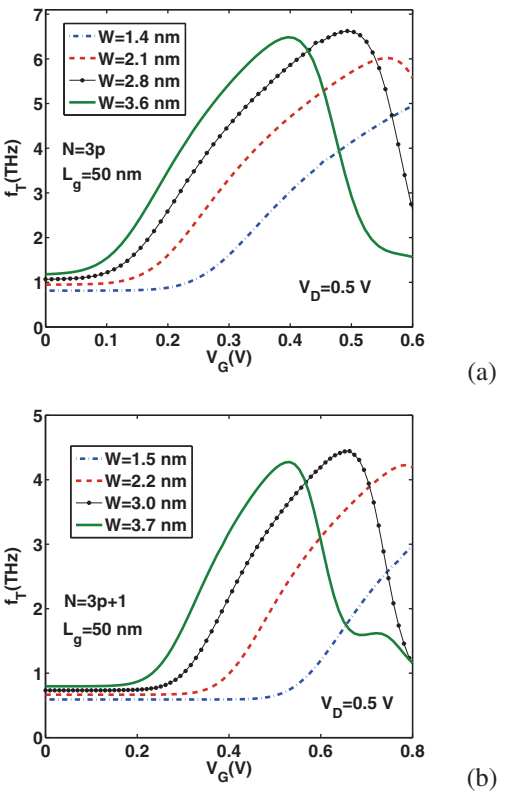

Fig. 5. f_T versus V_G characteristics for the families $N = 3p$ (a) and $N = 3p + 1$ (b), respectively. The channel length is taken as L_g=50 nm.

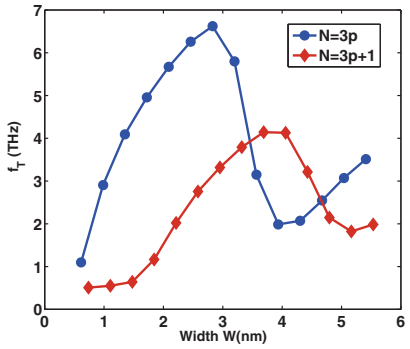

Fig. 6. Width dependence of the cut-off frequency for the two families $N = 3p$ and $N = 3p + 1$. The channel length is taken L_g=50 nm.

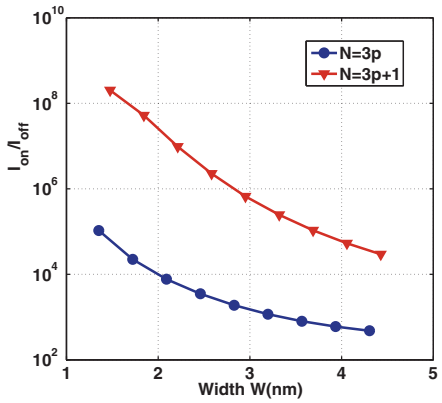

Fig. 7. Width dependence of I_{on}/I_{off} (b) for the two families $N = 3p$ and $N = 3p + 1$.

the family $N = 3p + 1$ seems to be the most suitable for switching applications. As it is seen, in order to obtain a ratio $I_{on}/I_{off} = 10^6$, (3p + 1)-AGNRs with widths of about 3-4 nm at most are required. Moreover, Fig. 8 shows the I_{on} versus I_{on}/I_{off} plots that provides a useful guide for selecting device characteristics that can yield the desirable I_{on}/I_{off} for a given I_{on}. As it is seen, reduction of GNR's width that leads to larger bandgap devices, can provide larger ratio I_{on}/I_{off} albeit at lower I_{on}. It should be noticed that, experimental

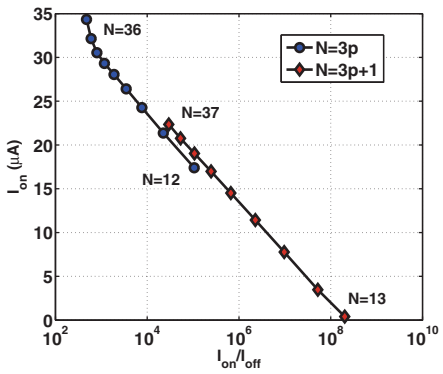

Fig. 8. Plots of I_{on} versus I_{on}/I_{off} for the two families $N = 3p$ and $N = 3p + 1$.

studies reported recently [12] support transistor action at room temperature with ratios I_{on}/I_{off} more than 10^6 in agreement with the above theoretical predictions.

IV. Conclusion

We have proposed a fully analytical model based on effective mass approximation and semiclassical ballistic transport to study the characteristics of AGNR-FETs. The model incorporates the effects of edge bond relaxation and third nearest neighbor interaction. The model is simple and computationally efficient with no iterations or numerical integration involved. Numerical results for a double-gate AGNR-FET with thin and high-κ gate-insulator, so that the QCL can be reached, are obtained. We have focused on the two AGNRs families with widths determined by $N = 3p$ and $N = 3p + 1$ with p a positive integer. Our calculations have shown that the transfer characteristics show smaller values of threshold voltage and larger drain currents for the group $N = 3p$ compared to those of the group $N = 3p + 1$ with approximately the same width. Throughout the bias window, the cutoff frequency f_T exceeds the THz barrier, confirming the excellent high-frequency potential of GNRs. Moreover, AGNRs with $N = 3p$ have higher maximum cutoff frequencies obtained at lower gate biases and hence, it might be preferable for high frequency applications. In order to obtain a ratio $I_{on}/I_{off} = 10^6$, $N = 3p + 1$-AGNRs with widths of about 3-4 nm at most are required. Finally, reduction of GNR's width that leads to larger bandgap devices, can provide larger ratio I_{on}/I_{off} albeit at lower I_{on}.

References

[1] A.H. Castro Neto, F. Guinea, N.R. Peres, K.S. Novoselov, A.K. Geim, "The electronic properties of graphene", *Rev. Mod. Phys.*, vol. 81, pp.109-162, 2009.

[2] Y.W. Son, M. Cohen, S. Louie, "Energy gaps in graphene nanoribbons", *Phys. Rev. Lett.* vol. 97, art. no. 216803, 2006.

[3] Y. Ouyang Y, Y. Yoon, J.K. Fodor, J. Guo, "Comparison of performance limits for carbon nanoribbon and carbon nanotube transistors", *Appl. Phys. Lett.*, vol. 89, art. no. 203107, 2006.

[4] P. Zhao and J. Guo, "Modeling edge effects in Graphene Nanoribbon Field-effect Transistors with real and mode space methods", *J. Appl. Phys.*, vol. 105, art. no. 034503, 2009.

[5] S. Fregonese, C. Maneux, Th. Zimmer, "A versatile compact model for ballistic 1D transistor: GNRFET and CNTFET comparison", *Solid State Electronics*, vol. 54, pp. 1332-1338, 2010.

[6] J. Knoch, W. Riess, and J. Appenzeller, "Outperforming the conventional scaling rules in the quantum capacitance limit", *IEEE Elect. Dev. Lett.*, vol. 29, no. 4, pp. 372-375, 2008.

[7] D. Gunlycke and C.T. White, "Tight-binding energy dispersions of armchair-edge graphene nanostrips", *Phys. Rev. B*, vol. 77, no. 16, art. no. 115116, 2008.

[8] G. S. Kliros, "Gate capacitance modeling and width-dependent performance of graphene nanoribbon transistors", *Microelectronic Engineering*, in press, 2013, http://dx.doi.org/10.1016/j.mee.2013.04.011

[9] J. Guo, Y. Yoon and Y. Ouyang, "Gate Electrostatics and Quantum Capacitance of GNRs" *Nano Lett.* vol. 7, no. 7, 1935-1940, 2007.

[10] K. Natori, "Compact modeling of ballistic nanowire MOSFETs", *IEEE Trans. Elect. Dev.*, vol. 52, no. 11, pp.501-503, 2008.

[11] G. S. Kliros, "Influence of density inhomogeneity on the quantum capacitance of graphene nanoribbon field effect transistors", *Superlattices and Microstructures*, vol. 52, pp. 10931102, 2012.

[12] X. Wang, *et al.* "Room-temperature all-semiconducting sub-10-nm graphene nanoribbon field-effect transistors", *Phys. Rev. Lett.* vol. 100, art. no. 206803, 2008.